

# Ligand Assisted Control of Photoluminescence in Organometal Perovskite Nanocrystals

K.S. Sekerbayev<sup>1</sup>, G.K. Mussabek<sup>1,2</sup>, Ye. Shabdan<sup>1</sup>, Ye.T. Taurbayev<sup>1\*</sup>

<sup>1</sup>Institute Experimental and Theoretical Physics, al-Farabi Kazakh National University,  
71 al-Farabi, Almaty, Kazakhstan

<sup>2</sup>Institute of Engineering Physics for Biomedicine, Laboratory “Bionanophotonics”, National Research Nuclear University “MEPhI”, 31 Kashirskoe shosse, Moscow, Russia

## Article info

*Received:*  
10 February 2021

*Received in revised form:*  
19 April 2021

*Accepted:*  
10 June 2021

### Keywords:

Perovskite  
Methylammonium  
Halides  
Photoluminescence  
Absorption spectroscopy

## Abstract

Organometal perovskite nanocrystals have shown remarkable properties not only in photovoltaics, but also in light-emitting devices. In this work colloidal nanocrystals of organometal perovskite  $\text{CH}_3\text{NH}_3\text{PbBr}_3$  (MAPBr) with effective visible photoluminescence were synthesized by the ligand assisted reprecipitation method. The studies were carried out by photoluminescence spectroscopy and optical transmission spectroscopy. Analysis of the photoluminescence and transmission spectra showed that by changing the concentration of the ligands oleylamine and octylamine, it is possible to control the size of nanocrystals and the photoluminescence wavelength due to the quantum confinement effect. It was shown that the increase in ligands concentration in MAPBr perovskite nanocrystals (NCs) solutions decreases the width of the peak which indicates a better quality of the obtained nanocrystals. An increase in the band gap indicates a decrease in the size of the nanocrystals. Replacing the ligands in the colloidal perovskite NCs solutions leads to shift of the photoluminescence peak from 456 to 535 nm.

## 1. Introduction

Over the past decade  $\text{ABX}_3$  (where  $\text{A} - \text{Cs}^+$ ,  $\text{NH}_2\text{CHNH}_2^+$  or  $\text{CH}_3\text{NH}_3^+$ ;  $\text{B} - \text{Sn}_2^+$  or  $\text{Pb}_2^+$ ;  $\text{X} - \text{Cl}^-$ ,  $\text{Br}^-$  or  $\text{I}^-$ ) organometal perovskites have shown rapid growth in optoelectronic applications. One of the best examples of such applications perovskites based solar cells, the efficiency of which increased from 3.8% to 25.5% by 2021 [1, 2]. Also, it is well known that perovskite nanocrystals have excellent light-emitting properties with a photoluminescence (PL) quantum yield of 90% [3, 4].

To date, there are two well-developed methods for the synthesis of colloidal nanocrystals of perovskites: the hot injection (HI) method and the ligand-assisted reprecipitation (LARP) method [5–7]. The HI method requires high temperatures and an inert atmosphere, which inevitably increases cost and can limit product yield in mass pro-

duction [8]. The LARP method allows to overcome mentioned limitations and could be considered as a less expensive alternative technique since it provides high quality perovskite nanocrystals (NCs) and synthesis occurs in the ambient atmosphere at room temperature [9].

The main idea of the LARP method is in dissolving the desired ions in a solvent reaching an equilibrium concentration and then bringing the solution into a non-equilibrium supersaturation state. The supersaturation state can be achieved by changing the temperature (cooling the solution), evaporating the solvent, or adding a co-solvent with low ions solubility. Under these conditions spontaneous precipitation and crystallization reactions occur until the system reaches equilibrium again. If this process is carried out in the presence of ligands, then it is called ligand-assisted reprecipitation. In this case, the formation and growth of crystals can be controlled down to the nanoscale which makes it possible to produce colloidal nanocrystals. It is

\*Corresponding author. E-mail: [taur@physics.kz](mailto:taur@physics.kz)

easy to understand that since the synthesis by the LARP method (as opposed to the HI methods) is carried out in air using a simple chemical apparatus it can be easily scaled. This advantage allows the organization the production of perovskite NCs in large quantities [10–12].

The first reports on LARP synthesis of hybrid organo-inorganic lead halide NCs date back to 2012 when Papavassiliou et al. dissolved salts of  $\text{CH}_3\text{NH}_3\text{PbX}_3$  (where  $X = \text{Br}, \text{Cl}, \text{ or } \text{I}$ ) in *N,N*-dimethylformamide (DMF) (or acetonitrile) and introduced this solution dropwise into toluene [13]. They observed the formation of luminescent NCs with sizes of 30–160 nm and photoluminescence intensity much higher than that expected for bulk  $\text{CH}_3\text{NH}_3\text{PbX}_3$  crystals. Several more years passed before the LARP procedure was finally developed for the synthesis of organic-inorganic nanocrystals. In this work, we performed the colloidal synthesis of methylammonium lead bromide perovskite NCs  $\text{CH}_3\text{NH}_3\text{PbBr}_3$  (MAPBr) with effective PL in the spectral range of 456–535 nm. We have optimized the process of synthesis of colloidal perovskite NCs and studied their photophysical properties.

## 2. Materials and methods

MAPBr perovskite NCs were synthesized by the colloidal LARP method. For perovskite systems the LARP method consists of adding precursor salts dissolved in a good polar solvent (DMF) to a poor solvent (for example, toluene or hexane) in the presence of ligands. For this, a solution of perovskite salts  $\text{CH}_3\text{NH}_3\text{PbBr}_3$  was prepared. 11.2 mg of  $\text{CH}_3\text{NH}_3\text{Br}$  and 36.7 mg of  $\text{PbBr}_2$  were dissolved in 1 ml of DMF. As a capping agent, i.e., ligands we have used oleic acid and various amounts of octylamine or oleylamine. 200  $\mu\text{l}$  of the oleic acid and different amounts of octylamine (15, 30, and 60  $\mu\text{l}$ ) were added in the solution with perovskite salt to obtain the first series of samples. The second series was prepared with the same solution, but instead of octylamine 15, 30, and 60  $\mu\text{l}$  of oleylamine were added.

In the next step, 100  $\mu\text{l}$  of prepared solution with perovskite salt and ligands (oleic acid and octylamine/oleylamine) were added to 3 ml of toluene with vigorous stirring. Mixing of two solvents causes instant supersaturation leading to the nucleation and growth of perovskite nanocrystals. In the process of stirring the solution acquired a green color and a greenish glow under ultraviolet light. Thus, colloidal nanocrystals of MAPBr perovskite

in toluene were obtained. In order to investigate the structural properties MAPBr NCs thin solid films were prepared from the colloidal solutions by spin-coating thin layers on silicon substrates and drying in a glovebox with 99.9% purity  $\text{N}_2$  atmosphere.

The structural morphology of MAPBr NCs films was characterized by Crossbeam 540 (Carl Zeiss) scanning electron microscope (SEM) and by JEM-1400 Plus (JEOL) transmission electron microscope (TEM). The optical properties of MAPBr perovskite NCs were studied by photoluminescence and optical transmission spectroscopy. PL spectra were measured using Carry Eclipse (Agilent) fluorescence spectrometer, transmittance spectra were measured using Lambda 35 (Perkin Elmer) spectrophotometer at room temperature.

## 3. Results and discussion

Figure 1 shows SEM and TEM images of MAPBr perovskite NCs with an average size 100 nm (inset) obtained by LARP method with 15  $\mu\text{l}$  oleylamine ligand. One can see that perovskite NCs are characterized by a cubic-like shape with average sizes of 5–130 nm for the samples prepared with different amounts of ligands.

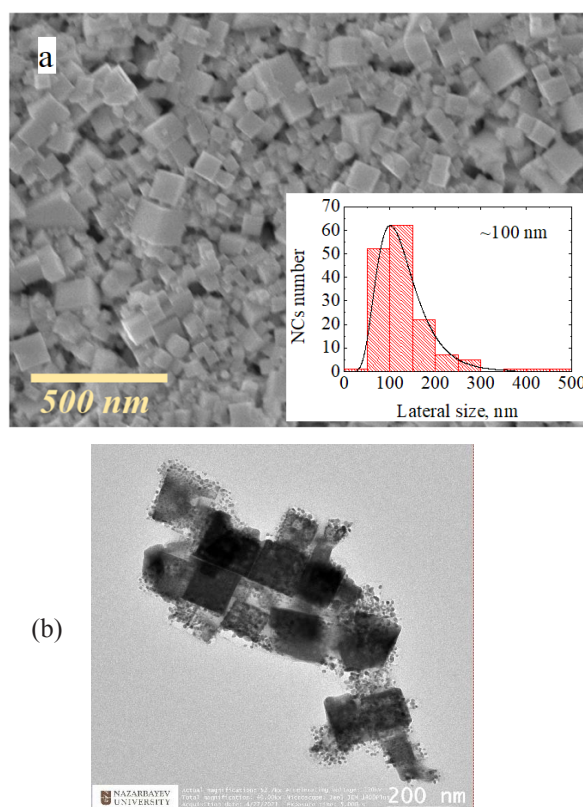


Fig. 1. (a) SEM and (b) TEM images of typical MAPBr perovskite NCs obtained by LARP method. Size distribution is shown in insets.

Organic ligands octylamine and oleylamine difference in effect on obtained perovskite NCs size are found by PL measurements. The PL spectra measurements showed the presence of a bright PL signal in all samples. Figure 2 shows the PL spectra of MAPBr nanocrystals with oleylamine. Figure 3 shows the transmission spectra of the same samples. One can see that the increase in the concentration of ligands shifts the luminescence peak to shorter wavelengths and decreases the width of the PL peak which is associated with a decrease in the size of nanocrystals. Two broad peaks are observed in the PL spectrum of the MAPBr perovskite NCs colloidal solution sample obtained at the concentration of 15  $\mu\text{l}$  of oleylamine. This means that at a low concentration of oleylamine crystals of large size with a large scatter are synthesized. This conclusion is confirmed by the

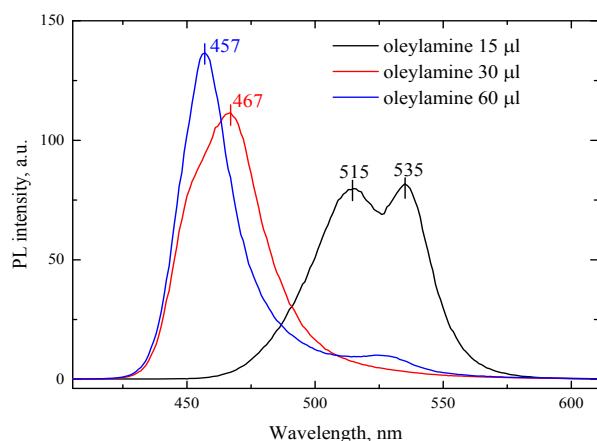


Fig. 2. Photoluminescence spectra of MAPBr perovskite NCs colloidal solutions in toluene with different concentrations of oleylamine. The excitation light wavelength is 300 nm.

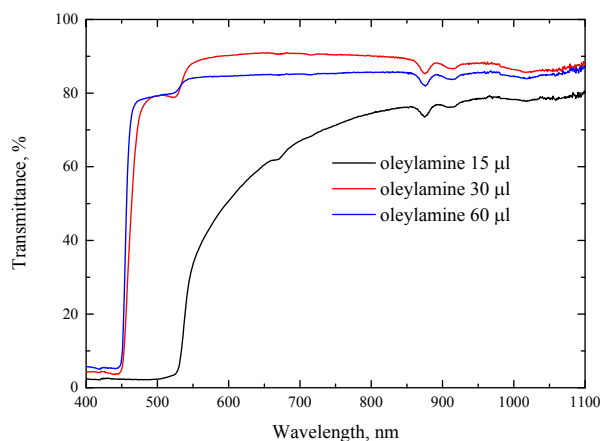


Fig. 3. Transmission spectra of MAPBr perovskite nanocrystals in toluene with different concentrations of oleylamine.

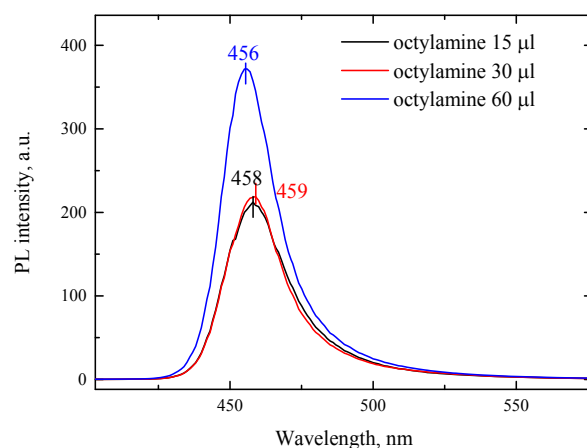


Fig. 4. Photoluminescence spectra of MAPBr perovskite NCs colloidal solutions in toluene with different concentrations of octylamine. The excitation light wavelength is 300 nm.

transmission spectrum which shows a diffuse absorption edge for the same sample.

Figure 4 shows the PL spectra of colloidal solutions of MAPBr nanocrystals in toluene synthesized with the addition of octylamine ligand. Samples of MAPBr nanocrystals synthesized using the octylamine ligand exhibit similar tendencies. However, 15  $\mu\text{l}$  and 30  $\mu\text{l}$  octylamine NCs show similar PL shape and intensity, 60  $\mu\text{l}$  of octylamine increases PL intensity two times. Even with a small amount of octylamine ligand MAPBr NCs show narrow PL spectra. This differs from oleylamine ligand effect.

Measurements of the transmission spectra of the same samples of MAPBr NCs (shown in Fig. 5) confirm the conclusions obtained from the analysis of the PL spectra. The transmission spectra have a sharp absorption edge coinciding with the PL peak for all octylamine concentrations.

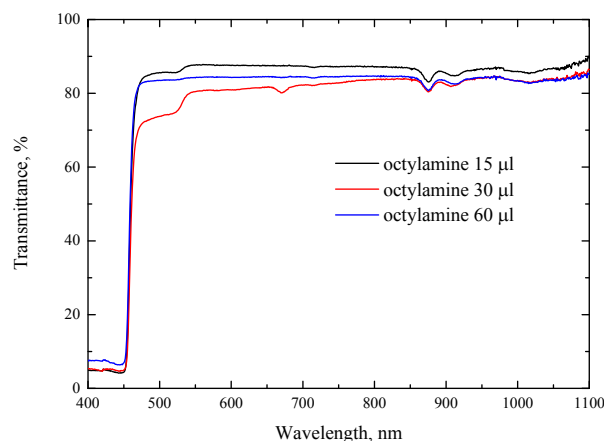


Fig. 5. Optical transmission of MAPBr perovskite NCs colloidal solutions in toluene with different concentrations of octylamine.

We can estimate the size and shape of synthesized NCs by comparing them with literature where the same method and perovskite composition are used. Same LARP technique with octylamine as ligand produces NCs with size 3.3 nm and PL peak at 515 nm [14]. In work [7] MAPBr NCs size and shape were analyzed, NCs have a plate shape, lateral size about 15 nm and thickness 3 nm. So, MAPBr NCs synthesized with a big amount of organic ligand have a plate shape and sizes lower than 20 nm.

The Bohr diameter for an exciton in perovskite is comparable to the size of nanocrystals which leads to the appearance of a quantum size effect in the form of an increase of band gap [15]. As a result, smaller nanocrystals emit shorter wavelength photoluminescence. According to the dependence of the energy of exciton transitions in MAPBr nanocrystals on the nanocrystal diameter known from the literature [16] the synthesized nanocrystals have a size less than 20 nm:

$$E_g^{NC} = E_g^{bulk} + \frac{h^2}{2d^2} \left( \frac{1}{m_e} + \frac{1}{m_h} \right)$$

where  $E_g^{NC}$  and  $E_g^{bulk}$  are band gap of nanocrystal and bulk MAPBr perovskite, respectively,  $m_e$  and  $m_h$  is the mass of electron and hole,  $d$  is the nanocrystal size.

Spread in the NCs diameters can be estimated from absorption edge shape and full width half maximum (FWHM) of PL spectrum. Sharper absorption edge (Figs. 3 and 5) and lower FWHM (Fig. 6b) indicates to narrow distribution of perovskite NCs diameters. Spread in the perovskite NCs sizes decreases with a larger amount of organic ligands. Organic ligands also cause an increase in the PL yield, which can be estimated from the area under the PL spectrum (Fig. 6a). In work [14]

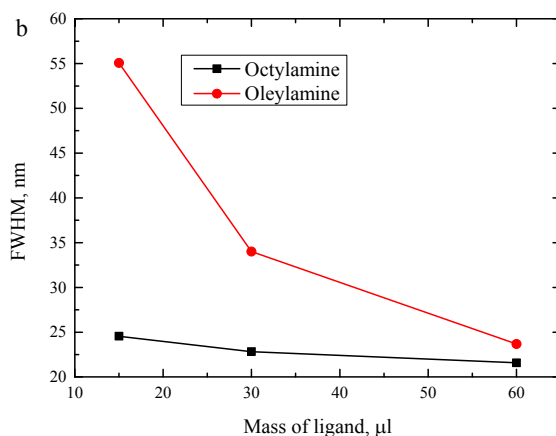
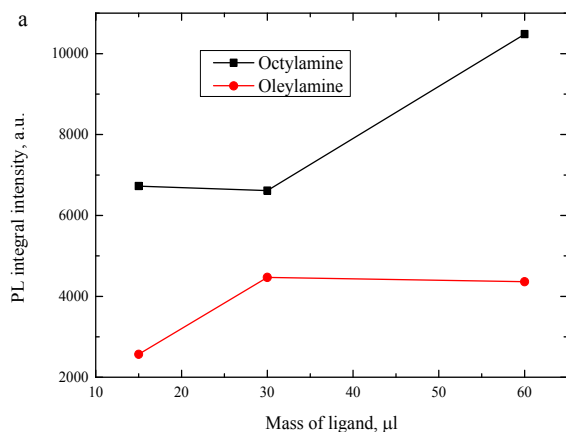


Fig. 6. (a) Integral PL intensity (b) Full width half maximum of PL spectrum of MAPBr perovskite NCs at different concentrations of ligands octylamine and oleylamine

MAPBr NCs obtained with the same method show PLQY in the range 50–70%. Therefore, using of octylamine is gives better results according to higher PL intensity and lower FWHM.

The comparison of characteristics of MAPBr perovskite NCs obtained at different concentrations of ligands are given in Tables 1 and 2 for octylamine and oleylamine, respectively.

**Table 1**

Position and half-width of the PL peak, band gap ( $E_g$ ) of MAPBr perovskite nanocrystals in toluene with different octylamine concentrations

Octylamine mass, μl	15	30	60
PL peak, nm	458	459	456
Half-width peak, nm	24.9	23.0	21.6
$E_g$ , eV	2.71	2.70	2.72

**Table 2**

Position and half-width of the PL peak, band gap ( $E_g$ ) of MAPBr perovskite nanocrystals in toluene with different concentrations of oleylamine

Oleylamine mass, μl	15	30	60
PL peak, nm	515, 535	467	457
Half-width peak, nm	57.0, 20.7	35.3	23.1
$E_g$ , eV	2.41, 2.32	2.66	2.71

## 4. Conclusions

Nanocrystals of organometal perovskite  $\text{CH}_3\text{NH}_3\text{PbBr}_3$  with bright photoluminescence have been obtained by low-cost and convenient LARP synthesis method. It was shown the possibility to control the photoluminescence region by changing

ligands concentration in the perovskite NCs solutions, without changing the composition of halogens in perovskite. By replacing the octylamine ligand with oleylamine and changing the concentration from 15 to 60  $\mu\text{L}$  the PL peak can be shifted from 535 to 456 nm. An increase in the band gap indicates a decrease in the size of the nanocrystals. High ligand concentration in a perovskite solution leads to better quality (uniformity and PL intensity) of the obtained nanocrystal. So, with an increase in ligands concentration nanocrystals with a smaller scatter of sizes and higher PL yield are obtained. In this case, octylamine ligand makes it possible to obtain brighter and more uniform perovskite NCs in comparison with oleylamine.

### Acknowledgements

This work was supported by the Ministry of Education and Science of the Republic of Kazakhstan (grant AP08052623).

### References

- [1]. A. Kojima, K. Teshima, Y. Shirai, T. Miyasaka, *J. Am. Chem. Soc.* 131 (2009) 6050–6051. DOI: [10.1021/ja809598r](https://doi.org/10.1021/ja809598r)
- [2]. Best Research-Cell Efficiency Chart. <https://www.nrel.gov/pv/cell-efficiency.html>
- [3]. G. Xing, N. Mathews, S.S. Lim, N. Yantara, X. Liu, D. Sabba, M. Grätzel, S. Mhaisalkar, T.C. Sum, *Nat. Mater.* 13 (2014) 476–480. DOI: [10.1038/nmat3911](https://doi.org/10.1038/nmat3911)
- [4]. Z. Xiao, R.A. Kerner, L. Zhao, N.L. Tran, K.M. Lee, T.-W. Koh, G.D. Scholes, B.P. Rand, *Nat. Photonics* 11 (2017) 108–115. DOI: [10.1038/nphoton.2016.269](https://doi.org/10.1038/nphoton.2016.269)
- [5]. H.C. Wang, Z. Bao, H.Y. Tsai, A.C. Tang, R.S. Liu, *Small* 14 (2018) 1702433. DOI: [10.1002/sml.201702433](https://doi.org/10.1002/sml.201702433)
- [6]. N. Wang, W. Liu, Q. Zhang, *Small Methods* 2 (2018) 1700380. DOI: [10.1002/smtd.201700380](https://doi.org/10.1002/smtd.201700380)
- [7]. I. Levchuk, P. Herre, M. Brandl, A. Osvet, R. Hock, W. Peukert, P. Schweizer, E. Spiecker, M. Batentschuk, C.J. Brabec, *Chem. Commun.* 53 (2017) 244–247. DOI: [10.1039/C6CC09266G](https://doi.org/10.1039/C6CC09266G)
- [8]. M.V. Kovalenko, L. Manna, A. Cabot, Z. Hens, D.V. Talapin, C.R. Kagan, V.I. Klimov, A.L. Rogach, P. Reiss, D.J. Milliron, *ACS Nano* 9 (2015) 1012–1057. DOI: [10.1021/mn506223h](https://doi.org/10.1021/mn506223h)
- [9]. X. Li, F. Cao, D. Yu, J. Chen, Z. Sun, Y. Shen, Y. Zhu, L. Wang, Y. Wei, Y. Wu, H. Zeng, *Small* 13 (2017) 1603996. DOI: [10.1002/sml.201603996](https://doi.org/10.1002/sml.201603996)
- [10]. J. Shamsi, P. Rastogi, V. Caligiuri, A.L. Abdelhady, D. Spirito, L. Manna, R. Krahn, *ACS Nano* 11 (2017) 10206–10213. DOI: [10.1021/acsnano.7b04761](https://doi.org/10.1021/acsnano.7b04761)
- [11]. S. Wei, Y. Yang, X. Kang, L. Wang, L. Huang, D. Pan, *Chem. Commun.* 52 (2016) 7265–7268. DOI: [10.1039/C6CC01500J](https://doi.org/10.1039/C6CC01500J)
- [12]. K.-H. Wang, L. Wu, L. Li, H.-B. Yao, H.-S. Qian, S.-H. Yu, *Angewandte Chemie* 128 (2016) 8468–8472. DOI: [10.1002/ange.201602787](https://doi.org/10.1002/ange.201602787)
- [13]. G.C. Papavassiliou, G. Pagona, N. Karousis, G.A. Mousdis, I. Koutselas, A. Vassilakopoulou, *J. Mater. Chem.* 22 (2012) 8271–8280. DOI: [10.1039/C2JM15783G](https://doi.org/10.1039/C2JM15783G)
- [14]. F. Zhang, H. Zhong, C. Chen, X.-G. Wu, X. Hu, H. Huang, J. Han, B. Zou, Y. Dong, *ACS Nano* 9 (2015) 4533–4542. DOI: [10.1021/acsnano.5b01154](https://doi.org/10.1021/acsnano.5b01154)
- [15]. D. Saponi, M. Kepenekian, L. Pedesseau, C. Katan, J. Even, *Nanoscale* 8 (2016) 6369–6378. DOI: [10.1039/C5NR07175E](https://doi.org/10.1039/C5NR07175E)
- [16]. A. Kirakosyan, J. Kim, S.W. Lee, I. Swathi, S. G. Yoon, J. Choi, *Cryst. Growth Des.* 17 (2017) 794–799. DOI: [10.1021/acs.cgd.6b01648](https://doi.org/10.1021/acs.cgd.6b01648)